

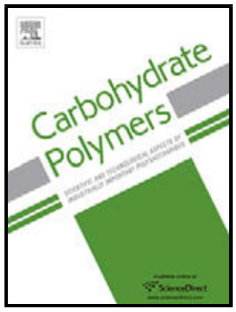


Title: Supramolecular structure of jackfruit seed starch and its relationship with digestibility and physicochemical properties

Author: Jin Chen Yi Liang Xiaoxi Li Ling Chen Fengwei Xie

PII: S0144-8617(16)30552-5
DOI: http://dx.doi.org/doi:10.1016/j.carbpol.2016.05.030
Reference: CARP 11099

To appear in:

Received date: 31-3-2016
Revised date: 27-4-2016
Accepted date: 11-5-2016

Please cite this article as: Chen, Jin., Liang, Yi., Li, Xiaoxi., Chen, Ling., & Xie, Fengwei., Supramolecular structure of jackfruit seed starch and its relationship with digestibility and physicochemical properties.*Carbohydrate Polymers* http://dx.doi.org/10.1016/j.carbpol.2016.05.030

# Supramolecular structure of jackfruit seed starch and its relationship with digestibility and physicochemical properties

Jin Chen [a], Yi Liang [b], Xiaoxi Li [a], Ling Chen [a,*] and Fengwei Xie [c,†]

[a] *Ministry of Education Engineering Research Center of Starch & Protein Processing, Guangdong Province Key Laboratory for Green Processing of Natural Products and Product Safety, School of Food Science and Engineering, South China University of Technology, Guangzhou, Guangdong 510640, China*

[b] *Guangdong Zhongqing Font Biochemical Science and Technology Co. Ltd., Maoming, Guangdong 525427, China*

[c] *School of Chemical Engineering, The University of Queensland, Brisbane, Qld 4072, Australia*

[*] Corresponding author. Tel.: +86 20 8711 3252; fax: +86 20 8711 3252. *Email address:* felchen@scut.edu.cn (L. Chen)

[†] Corresponding author. Tel.: +61 7 3346 3199; fax: +61 7 3346 3973. *Email addresses:* f.xie@uq.edu.au, fwhsieh@gmail.com (F. Xie).

**ABSTRACT**

The influence of supramolecular structure on the physicochemical properties and digestibility of jackfruit seed starch (JSS) were investigated. Compared with maize and cassava starches (MS and CS), JSS had smaller granules and higher amylose content (JSS: 24.90%; CS: 16.68%; and MS: 22.42%), which contributed to higher gelatinization temperature ($T_o$: 81.11°C) and setback viscosity (548.9 mPa·s). From scanning electron microscopy, the digestion of JSS was observed mainly at the granule surface. Due to its higher crystallinity (JSS: 30.6%; CS: 30.3%; and MS: 27.4%) and more ordered semi-crystalline lamellae, JSS had a high RS content (74.26%) and melting enthalpy (19.61 J/g). In other words, the supramolecular structure of JSS extensively determined its digestibility and resistance to heat and mechanical shear treatment.

*Keywords:*

Jackfruit seed starch; Supramolecular structure; Resistant starch; Digestibility; Thermal properties

**Highlights:**

- ✓ Jackfruit seed starch (JSS) had higher resistant starch content than other starches
- ✓ High crystallinity and ordered semi-crystalline lamellae were the major reasons for the higher enzyme-resistance of JSS
- ✓ Digestion of JSS occurred mainly at the granule surface
- ✓ Digestion caused slight decrease in crystallinity and lamellar regularity of JSS

Chemical compounds studied in this article

Starch (PubChem CID: 24836924); Sodium hydroxide (PubChem CID: 14798); Water (PubChem CID: 962); Hydrochloric acid (PubChem CID: 313); Ethanol (PubChem CID: 702); Acetic acid (PubChem CID: 176); Iodine (PubChem CID: 807); Potassium iodine (PubChem CID: 4875); Sodium acetate (PubChem CID: 517045).

## 1. Introduction

Starch is one of the most important carbohydrates in human diets and has been extensively used as a food ingredient. Understanding starch digestibility is of great interest to food industry and importance for diet-related disorders such as obesity, diabetes, and cardiovascular diseases. Not all starch can be digested in the small intestine, where the portion of starch that is not digested is termed resistant starch (RS) (Asp & Björck, 1992). Physiological benefits have been correlated to the RS consumption (Englyst & Hudson, 1996; Jenkins et al., 1998), which notably alters fecal bulk and short-chain fatty acid metabolism, thus promoting the colonic health (Jenkins et al., 1998).

Because hydrolysis influences all level of food processing and nutrition, several arguments prevail for a closer examination of the effects of hydrolytic enzymes on native starch granules. The hydrolysis process of starches includes the diffusion of enzymes to the granule surface, followed by the adsorption and subsequent catalytic events (Colonna, Leloup & Buleon, 1992). Previous studies have shown that the action of α-amylase on starches from different botanical origins results in varied digestion kinetics and degradation patterns (Fuwa, Takaya, Sugimoto & Marshall, 1980;

Sarikaya, Higasa, Adachi & Mikami, 2000). Generally, starch is a mixture of two types of macromolecules, amylose and amylopectin (Hizukuri, 1985). Double or single helices of amylose and amylopectin can be packed to form amorphous and crystalline regions (Oates, 1997), which is the basis of the supramolecular structure (granule morphology, fractal structure, lamellar structure, and crystalline structure) of starch. There are many structural factors of starch that affect the pattern and rate of enzymatic hydrolysis, such as the size and shape of granules, granule integrity, porosity of granules, crystallinity, amylose/amylopectin ratio, phosphate content, proteins, and lipids on the granule surface (Copeland, Blazek, Salman & Tang, 2009; Dona, Pages, Gilbert & Kuchel, 2010; Planchot, Colonna, Gallant & Bouchet, 1995; Robertson, Wong, Lee, Wagschal, Smith & Orts, 2006; Tester, Qi & Karkalas, 2006). The features of native starch granules that control the site, rate and extent of hydrolysis by α-amylase are interrelated and not easily definable. Thus, studying the changes of supramolecular structure would help to build the ability to manipulate and understand the hydrolysis of starch granules.

Jackfruit is one of the most popular tropical fruits grown in Asia especially in Thailand. Its seeds take up 10–15% of the whole fruits and contain abundant starch and proteins. With the rapid development of the cultivating and processing industry of jackfruit, however, most seeds are discarded, which causes a huge waste of starch resource. Jackfruit seed starch has not been considered and exploited as a potent source of starch. To solve this problem, there have been studies on the isolation and the properties of starch extracted from jackfruit seeds to verify its applicability in food, pharmaceutics and other uses. Jackfruit seed starch has the Type-A crystallinity pattern and a high amylose content (Madruga, de Albuquerque, Silva, do Amaral, Magnani & Neto, 2014). Compared with other starches, jackfruit seed starch has significantly higher gelatinization

101 temperature and lower breakdown viscosity, suggesting that this starch can be used to products
102 where a high level of gelatinization is not desirable during cooking (Bobbio, EI-Dash, Bobbio &
103 Rodrigues, 1978; Kittipongpatana & Kittipongpatana, 2011; Rengsutthi & Charoenrein, 2011;
104 Theivasanthi & Alagar, 2011; Tulyathan, Tananuwong, Songjinda & Jaiboon, 2002; Yi &
105 Shenghong, 2006). However, the literature provides little information about the structural features
106 of jackfruit seed starch and its effects on different properties. In particular, while the supramolecular
107 structure and its effect on the hydrolysis of native jackfruit seed starch are essential to ensure the
108 nutritional value and a diverse range of food industry uses, this information has not been reported so
109 far.

110 The aim of the present study was to investigate the functional properties and enzyme digestion
111 of jackfruit seed starch, as well as the related hierarchical structure changes in the native starch
112 granule that control the susceptibility of starch to enzymatic hydrolysis. The results of jackfruit seed
113 starch were compared with cassava starch and maize starch, which are two of the most popular
114 starches used in food industry. This would provide us with nutritional implications which are
115 instrumental for practical applications.

116

117 **2. Materials and methods**

118 *2.1. Materials*

119 Jackfruit Seed Starch (JSS) was isolated from jackfruit seeds using a modified method of
120 (Bobbio, EI-Dash, Bobbio & Rodrigues, 1978). The seeds were manually separated from the
121 mucilage, and then the aril and spermoderm were peeled off. The peeled seeds were slurried in a
122 Waring Blender (HR 1727 Philips, Zhuhai, China) with an equal weight of a 0.1% sodium

hydroxide solution for approximately 10 min. Then, the slurry was pressed through multiple gauzes to remove seed fibers. The resulting milking suspension was allowed to decant at 4−5°C and rewashed with distilled water to eliminate soluble sugars. The supernatant was drained, and the upper brown sediment was scraped. The remaining sediment was mixed with 0.1% sodium hydroxide solution and filtered through a sieve (0.058 mm mesh size) to eliminate fibers. When the supernatant became clear, the filtrate was neutralized with 0.1M hydrochloric acid to pH 7.0, and the slurry was centrifuged at 3,000 g for 20 min. The starch was dried at 40°C for 24 h. The starch was grounded with a mortar, passed through a sieve (0.15 mm mesh size), packed in a plastic bag and kept at room temperature until further use. The yield of JSS from Jackfruit seed was 25.45–27.34 g/100 g (dry basis).

Cassava starch (CS) was purchased from Vietnamese Food and Investment Co., Ltd. (Nanning, China). Maize starch (MS) was from Inner Mongolia Wang Yu Biotechnology Co., Ltd. (Inner Mongolia, China). The moisture contents of JSS, CS, and MS, determined using a moisture analyzer (DHS20-1, Sartorius Stedim Biotech GmbH, Germany), were 13.03%, 13.44%, and 13.25%, respectively. Porcine pancreatic α-amylase and amyloglucosidase were purchased from Sigma-Aldrich (St. Louis, MO, USA). A glucose-oxidase peroxidase (GOPOD) assay kit was from Megazyme International Ireland, Ltd. (Wicklow, Ireland). Potato amylose was purchased from Heilongjiang Academy of Agricultural Sciences (Harbin, China).

### *2.2. Starch characterization*

#### *2.2.1. Amylose content analysis*

The RS content of each sample (JSS, CS, and MS) was determined using a modified method of

ISO 6647-2:2007, of the International Standardization Organization (ISO, 2007).

0.1 g of the starch (dry basis) was accurately weighed and dissolved in 1 ml of ethanol and 9 ml of sodium hydroxide solution (1 M), then heated in boiling water for 10 min. After cooling off, this solution was then diluted to 100 mL in a volumetric flask with deionized water. An aliquot (2.50 mL) of this solution was then diluted with 25.00 mL of water, 0.50 mL of acetic acid solution (1 M), 0.50 mL of $I_2$/KI solution (0.0025 M $I_2$, and 0.0065 M KI), and the absorbance of this solution was read in a 1cm path length quartz cell at 620 nm using an Evolution UV/Visible spectrophotometer (Thermo Scientific, Waltham, USA). The amylose from potato (amylose content: 97.0%) was used for the calibration curve ($R^2$=0.9962).

*2.2.2. Differential scanning calorimetry (DSC)*

Thermal behaviors of JSS, CS, and MS were studied using a PerkinElmer DSC 8000 (PerkinElmer, Waltham, America) with an internal coolant (Intercooler 2P) and nitrogen purge gas. A high-pressure stainless steel pan (PerkinElmer No. B0182901) with a gold-plated copper seal (PerkinElmer No. 042-191758) was used to achieve a constant moisture content (MC) during DSC measurements. The sample, with about 70% MC, was prepared by premixing the starch with added water in a sealed glass vial, which was kept at 20°C for 24 h before measurement. About a 4 mg (dry basis) sample, scanned from 40 to 120°C, was used in this study. A slow heating rate of 5°C/min was used. The onset temperature ($T_o$), peak temperature ($T_p$), conclusion temperature ($T_c$), and enthalpy ($\Delta H$) of starch gelatinization were calculated. The enthalpy was calculated based on the weight of dry basis starch.

### *2.2.3. Pasting properties*

Pasting properties were studied using an Anton Paar MCR302 (Anton Paar China, Shanghai, China). The sample slurry (6% concentration, starch on dry basis), after 1 min pre-shearing, was heated from 30°C to 95°C at a heating rate of 5°C/min, held at 95°C for 15 min, and cooled to 50°C at 5°C/min. Then the sample was held at 50°C for 15 min. The changes of viscosity were recorded.

## *2.3. Enzyme digestion of starches*

### *2.3.1. In vitro digestibility of native starches*

For native JSS, CS, and MS, the starch digestibility was determined following the modified method of Englyst (Englyst, Kingman & Cummings, 1992). Based on the rate of hydrolysis, starch was defined as rapidly-digestible starch (RDS, digested within 20 min), slowly-digestible starch (SDS, digested between 20 min and 120 min), and resistant starch (RS, undigested within 120 min).

In brief, porcine pancreatic α-amylase (3 g) was dispersed in water (20 mL), stirred for 10 min and centrifuged at 3000 g for 15 min. The supernatant (13.5 mL) was transferred to a beaker, and 225 U of amyloglucosidase and 1 mL of deionized water were added to the solution. The enzymatic solution should be freshly prepared for each digestion. Duplicate samples (one named Sample A, the other Sample B) of each starch (JSS, CS, and MS) (1 g, dry basis) were dispersed in 20 mL of 0.1 M sodium acetate buffer (pH = 5.2) and then mixed with an enzyme solution (5 mL) consisting of the pancreatic extract and amyloglucosidase. The dispersion was incubated in a 37 °C shaking water-bath at 180 strokes/min. An aliquot (0.5 mL) of Sample A was taken at interval of 20 min and mixed with 20 ml of 70% ethanol. The mixed solution of Sample A was centrifuged at 3000 g for 10 min, and then the supernatant was used for hydrolyzing the glucose content, measured by the

glucose oxidase-peroxidase reagent. Sample B was mixed with ethanol to eliminate the activities of enzyme, and then the dispersion was centrifuged at 3,000 g for 20 min. After three times of mixing with ethanol and centrifugation, the sediments of Sample B were dried at 40°C for 12 h, named JSS-20, CS-20, and MS-20 ("20" means the time interval (min) for which the three starches were hydrolyzed), respectively. When the time interval reached 120 min, another aliquot (0.5 mL) of Sample A was taken and mixed with 20 ml of 70% ethanol, centrifuged to analyze the hydrolyzed glucose content. The sediments were treated using the same method of Sample B. These sediments were JSS-120, CS-120, and MS-120, respectively.

*2.3.2. Scanning electron microscopy (SEM)*

Granule morphology was studied using an EVO18 scanning electron microscope (ZEISS, Germany) operated at a high voltage of 10.0 kV. Before the SEM examination, the samples were coated with a gold thin film.

*2.3.3. Small-angle X-ray scattering (SAXS)*

A SAXSess small angle X-ray scattering system (Anton Paar, Austria), operated at 50 mA and 40 kV, using Cu Kα radiation with a wavelength of 0.1542 nm as the X-ray source, was applied to perform the SAXS measurements according to our previously method (Zhu, Li, Chen & Li, 2012) with proper modification. Each sample was placed in a paste sample cell and exposed at the incident X-ray monochromatic beam for 10 min. The data, recorded using an image plate, were collected by the IP Reader software with a PerkinElmer storage phosphor system.

The samples used for the SAXS measurement were prepared by premixing the starch with added water in glass vials and were equilibrated at 20°C for 24 h before the analysis. The total MC

of each sample was 65%. All data were normalized, and the background intensity and smeared intensity were removed using the SAXSquant 3.0 software for further analysis.

*2.3.4. Polarized light microscopy*

Polarized light microscopy was performed using a polarized light microscope (PLM) (Axioskop 40 Pol/40A Pol, ZEISS, Oberkochen, Germany) equipped with a 35mm SLA camera (Power Shot G5, Canon, Tokyo, Japan). The magnification was 500 (50×10). Each sample was dispersed as 10 mg (wet basis) of starch in 1 mL of distilled water in a glass vial. Then, a drop of the starch suspension was transferred onto a slide and covered by a coverslip. Polarized light was used for observation.

*2.3.5. X-ray diffraction (XRD)*

XRD analysis was performed with an Xpert PRO diffractometer (Panlytical, Netherlands), operated at 40 mA and 40 kV, using Cu Kα radiation with a wavelength of 0.1542 nm as the X-ray source. The scanning of diffraction angle ($2\theta$) was from 5° to 40° with a scanning speed of 10°/min and scanning step of 0.033°. The MC of each sample was about 10%. The relative crystallinity of each sample was calculated using a previous method (Hermans & Weidinger, 1948).

*2.4 Statistical analysis*

The mean values and differences were analyzed using Duncan's multiple-range test. Analysis of variance (ANOVA), followed by the least significant difference test (LSD-test), was performed using the software SPSS (Version 22.0). The significance level was set at $p < 0.05$.

## 3. Results and discussion

### *3.1. Amylose contents and in vitro enzyme digestion analysis of native starches*

The amylose/amylopectin ratio is an important index of starch and it can influence digestion and swelling properties through the way of amylose and amylopectin packed. As seen from Table 1, compared to CS and MS, the amylose content of JSS was higher (24.90%), which was similar to a previous finding (Li & Zhong, 2004). CS had the lowest amylose content, only 16.68%. Based on the Englyst test, the percentages of RDS, SDS, and RS in JSS were 5.92%, 19.82%, and 74.26%, respectively. The RS content of JSS was much higher than CS and MS while RDS and SDS were lower, indicating that JSS had strong anti-enzymatic capability. Interestingly, MS had the lowest RS content but the highest SDS content, suggesting that it is a good material of SDS. The slow-digestion property of MS is more likely to be controlled by its inherent structure (perhaps amylopectin chain length distribution) although the existence of surface porous channels might contribute to a high rate of starch hydrolysis (Zhang, Ao & Hamaker, 2006).

### *3.2. Supramolecular structure characteristics of native and hydrolyzed starches*

#### *3.2.1. Granule morphology*

Fig. 1 shows the SEM images of JSS, CS and MS in their native states and after 20min and 120min enzyme hydrolysis. The JSS and CS granules had round to bell shapes with a smooth surface. Unlike the other two starches, the MS granules were irregular in shape with small pores and

255 pits randomly distributed on a rough surface. The JSS granules were less irregular in shape, being
256 smaller than the CS and MS granules.
257
258
259
260 The susceptibility of starch granules can be classified by the degree and manner by which the
261 granules are eroded and corroded. As seen from SEM, the degree of digestion of starch followed the
262 order: MS > CS > JSS, contrary to the trend of RS (Table 1), which is as expected. Besides, the
263 observed levels of digestion were comparable between large and small granules for all three raw
264 starches. Some small granules in JSS-20 and CS-20 even became hollow with only a thin external
265 shell structure. This suggests a fundamental difference in the mode of α-amylase and
266 amyloglucosidase action, according to the granule size. Smaller granules, by virtue of their higher
267 available surface area per unit mass, facilitate the diffusion and adsorption of enzymes (Colonna,
268 Leloup & Buleon, 1992).
269 Digestion of JSS was not clearly apparent; the main indication was a less smooth and more
270 rugged granule surface with a few pits (JSS-20 and JSS-20, in Fig.1). Enzymatic digestion of CS
271 was apparent from the increased surface roughness and formation of deep cracks and large holes in
272 many granules (CS-20 and CS-120 in Fig.1). After 20min of enzymatic digestion, some CS granules
273 were in a truncated form (CS-20 in Fig.1). Truncatures are weak points in the granule structure that
274 lead to increased susceptibility, resulting in enhanced hydrolysis of CS. (Valetudie, Colonna,
275 Bouchet & Gallant, 1993). Because of no pores and smooth surfaces, SEM micrographs for JSS and
276 CS showed that enzymatic erosion occurred mainly at the surface. The MS granules showed

277 extensive corrosion, mainly in the direction of the radial axis and only a few granules remained
278 intact. The surface pores of hydrolyzed MS became larger and deeper into granules because of the
279 more extensive hydrolysis (MS-20 in Fig.1). After 120min hydrolysis, some granules were split,
280 exposing their layered internal structure (MS-120 in Fig.1). The layered internal structure showed
281 different susceptibility of the semi-crystalline structure and amorphous growth rings toward
282 digestion (Zhang, Ao & Hamaker, 2006).
283
284 *3.2.2. Lamellar structure characteristics*
285 The double-logarithmic SAXS patterns of native and hydrolyzed starch residues are shown in
286 Fig. 2. From this figure, we can obtain some parameters of a theoretical model for the lamellar
287 structure in starch (Cameron & Donald, 1993a, b), including $d$, the average thickness of the
288 semi-crystalline lamellae; $\Delta\rho = \rho_c - \rho_a$ (where $\rho_c$ and $\rho_a$ are the electron densities of the crystalline
289 regions and the amorphous regions in the semi-crystalline lamellae), the difference in electron
290 density between the crystalline lamellae and the amorphous lamellae; $\Delta\rho_u = \rho_u - \rho_a$ (where $\rho_u$ is the
291 electron density of the amorphous background), the difference in election density between the value
292 of $q$ of the peak at *ca.* 0.6 $nm^{-1}$ can be used to calculate the average repeat distance ($d$) of the
293 semi-crystalline lamellae in starch granules according to the Woolf-Bragg's equation $d = 2\pi/q$
294 (Blazek & Gilbert, 2010; Vermeylen, Goderis & Delcour, 2006). Table 2 shows the SAXS
295 parameters from the peaks of native and hydrolyzed starches. It can be seen from Table 2 that the
296 average thickness of the semi-crystalline lamellae of JSS and CS were thinner than that of MS (JSS:
297 9.06 nm; CS: 9.14 nm; and MS: 9.42 nm) and the peak areas of JSS and CS were larger than MS
298 (JSS: 0.1288; CS: 0.1248; and MS: 0.0800). This indicates JSS and CS may have more ordered

semi-crystalline lamellae than MS.

The log $I \sim \log q$ SAXS patterns of JSS, CS, and MS and their hydrolyzed residues are presented in Fig. 2a, b and c. The scattering intensity changed slightly for JSS (JSS-20 and JSS-120 in Fig. 2a) during the whole enzymatic hydrolysis. After 120min hydrolysis, the scattering intensity at the low $q$ region showed an increasing trend (JSS-120 in Fig. 2a) and the definition of the peak of JSS-120 was lower than those of JSS and JSS-20. This can be explained by the easier disturbance of starch molecular arrangement in the amorphous background than in the amorphous lamellae by α-amylase, thus resulting in an increase in $\Delta\rho_u$ (Cameron & Donald, 1992). All the analysis of JSS showed that most of the semi-crystalline lamellae of JSS remained intact even after 120min hydrolysis. And the slight changes in the scattering intensity of JSS, JSS-20, and JSS-120 explained a high RS content of JSS and less obvious surface erosion. However for CS and MS (CS-20 in Fig. 2b and MS-20 in Fig. 2c), the $q$ region around the peak showed a decreasing trend, suggesting the crystalline regions in the semi-crystalline lamellae were disturbed after 20min hydrolysis. And the scattering intensity at the low $q$ region showed an increasing trend, due to more destruction to the amorphous background than to the amorphous lamellae. After 120min hydrolysis (CS-120 in Fig. 2b and MS-120 in Fig. 2c), the scattering intensity decreased to an extensive degree. It is noted that the decrease of scattering intensity in MS was faster during the first 20 min of enzymatic hydrolysis and slower from 20 min to 120 min than in CS. This could be an excellent explanation for the higher SDS content of MS. Based on the above discussion, a conclusion can be made that the

321 semi-crystalline lamellae of JSS were more ordered and thus more resistant to the hydrolysis than
322 those of CS and MS.
323
324 *3.2.3 Crystalline characteristics*
325 Normally, a birefringence cross can be observed when the starch granule is exposed under
326 polarized light, due to orderly-arranged starch molecules of crystalline regions and
327 disorderly-arranged starch molecules of amorphous regions. Therefore, information about the
328 crystalline structure of starch can be reflected by the birefringence pattern when starch granules
329 suffered from hydrolysis or external attack. The polarized light microscope images of JSS, CS, and
330 MS and their hydrolyzed residues are shown in Fig. 3. Given the different sizes of JSS, CS, and MS
331 granules, native JSS showed weaker birefringence intensity than CS and MS, while CS showed the
332 strongest intensity. It is noted that the birefringence intensity remained almost the same for JSS after
333 enzyme hydrolysis for 120 min, suggesting most of crystalline structure of JSS was retained.
334 Nevertheless, the birefringence intensity decreased significantly for CS and MS (especially for MS),
335 and the birefringence crosses became less apparent, owing to the disturbance of double helices in
336 their crystallites during enzyme digestion. This result is consistent with the analysis of SAXS.
337
338
339
340 Fig. 4 shows the XRD patterns of JSS, CS, and MS, and their hydrolyzed residues. It is seen
341 that JSS and MS displayed a typical A-type crystalline structure with main diffraction peaks at *ca.*
342 15, 17, 18 and 23° (2$\theta$) (Tulyathan, Tananuwong, Songjinda & Jaiboon, 2002; Zobel, 1964). CS

exhibited a weak diffraction maximum at 5.6°(2$\theta$), and the 17°(2$\theta$) peak was somewhat more intense than its 18° (2$\theta$) neighbor (Chrastil, 1987). Both features indicated CS contained some B-type crystalline structure but the main structure was still A-type. The degree of relative crystallinity of starch followed the order: JSS ≈ CS > MS. According to the XRD patterns of partly-digested starches of JSS, CS and MS, the crystalline types of all three starches remained essentially unchanged after digestion. However, after enzyme treatment, decreased diffraction intensities were observed (Figure 4a, b, and c). The relative crystallinity of JSS changed moderately, decreased from 30.6% to 27.6% (Table 2) after 20min digestion, while CS and MS decreased more sharply from 30.3% to 23.6% and 27.4% to 19.4%, respectively. These results suggest that hydrolysis did occur in the crystalline regions despite that most of crystalline structure of JSS was retained after 120min hydrolysis.

It is noted that although JSS and CS both had a smooth surface and similar relative crystallinity (Table 2), the RS content of JSS was higher than CS. This can be demonstrated by the observation that the degree of the ordered structure in semi-crystalline lamellae was in the order JSS・CS・MS in the SAXS, suggesting not only the crystallinity but the way how molecules are ordered play a key role in the enzyme digestion of JSS. Another reason could be due to their amylose/amylopectin ratio. Specifically, a higher amylose content may mean an increased number of long chains and facilitate the amylose-lipid complex formation on the granule surface, leading to an increased content of enzyme-resistant starch (Crowe, Seligman & Copeland, 2000; Cui & Oates, 1999; Tufvesson, Skrabanja, Björck, Elmståhl & Eliasson, 2001). The surface pores and low relative crystallinity of MS could contribute to its high RDS and low RS contents.

When the α-amylase attacks starch granules, the double helices must first be unwound, as single-stranded helices are the polymeric substrates for the enzyme (Larson, Day & McPherson, 2010). The amylopectin double helices can only be unwound if they are dissociated from their crystallites. However, the amylopectin side chains of starch strongly interact, not only with their helical duplex partners, but also with other neighboring helices. Thus, more ordered crystalline structure leads to a lower rate of enzymatic hydrolysis because of stronger interactions between neighboring helices. Normally, higher crystallinity is in consistent with more ordered arrangement of amylopectin double helices in the semi-crystalline lamellae, since the crystallinity reflects the long range order of starch. In the light of these principles, the more ordered crystalline structure (corresponding to more ordered semi-crystalline lamellae and high relative crystallinity) was the main reason for the strong anti-enzymatic capability of JSS.

### *3.3. Thermal behavior*

Fig.5a shows the DSC thermograms of JSS, CS and MS in excess water (70 wt.%) and the related thermal parameters were shown in Table 3. From Fig.5a and Table 3, it was obvious that JSS had the highest gelatinization temperature ($T_o$: 81.11°C), followed by MS ($T_o$: 65.58°C) and CS ($T_o$: 60.47°C). The higher $T_o$, $T_p$, and $T_c$ of JSS could be due to a higher content of amylose-lipid complexes with an increased amylose content, resulting in reduced swelling of the granule (Karkalas & Raphaelides, 1986; Pycia, Juszczak, Gałkowska & Witczak, 2012; Svihus, Uhlen & Harstad, 2005; Tester & Morrison, 1990). The higher gelatinization temperature of JSS may also reflect its much longer amylopectin chains, as there is a significant positive correlation between the DSC gelatinization parameters and the amylopectin unit-chain length distribution of starches (Jane

et al., 1999; Noda et al., 1998; Shi & Seib, 1995; Srichuwong, Sunarti, Mishima, Isono & Hisamatsu, 2005a). Since the granule size followed the order CS‧ MS‧ JSS (Fig.1), another reason could be related to the size of starch granules since larger granules might be more vulnerable during heating (Chiotelli & Le Meste, 2002; Kaur, Singh & Sodhi, 2002; Vasanthan & Bhatty, 1996). JSS and MS showed rather symmetric peaks and had similar $\Delta T$, which was narrower than that of CS. This indicates that the crystalline structure of JSS and MS are more unified and consistent than that of CS, resulting in more homogeneous heat conductivity. Higher $\Delta T$ of CS was proposed to arise from the inconsistency of crystalline structure corresponding to the melting of B-type in CS although the main structure in CS was A-type. JSS and CS had similar $\Delta H$ (Table 3), due to their similar relative crystallinity, which were higher than that of MS.The higher $\Delta H$ values suggested that the interactions (via hydrogen bonding) between double helices (which were packed in clusters) forming the crystalline regions of JSS and CS were probably more extensive than in MS (Cooke & Gidley, 1992; Zhou, Hoover & Liu, 2004).

### *3.4. Pasting properties*

Fig.5b shows the pasting properties of JSS, CS and MS. As seen from Table 3, the peak viscosity (PV) of three starches followed the order JSS‧ CS‧ MS, which corresponded to the trend of $T_o$. The breakdown viscosity (BDV) of JSS (109.5 mPa·s) was lower than those of CS and MS

(473.2 mPa·s and 288.4 mPa·s, respectively). When viscosity reached PV, almost all of amylose leached out and therefore BDV was less affected by amylose, but more by amylopectin fine structure (Han & Hamaker, 2001). Lower BDV is another indicator that JSS may have much longer amylopectin chains since dissociation of double helices of amylopectin leads to granule swelling and affects pasting properties to some extent (Han & Hamaker, 2001; Srichuwong, Sunarti, Mishima, Isono & Hisamatsu, 2005b). The final viscosity (FV) and setback viscosity (SBV) indicate the re-association of the starch molecules involving amylose after gelatinization and a formation of a gel network (Charles, Chang, Ko, Sriroth & Huang, 2004). JSS had higher FV and SBV than CS and MS (Table 3), owing to a high amylose content (Sasaki, Yasui & Matsuki, 2000; Vandeputte, Derycke, Geeroms & Delcour, 2003). The reason CS had less amylose content but higher FV and SB than MS might be due to the finer amylopectin structure (enrichment in B2 chains) of CS (Srichuwong, Sunarti, Mishima, Isono & Hisamatsu, 2005b).

## 4. Conclusion

JSS granules were shown to be small, round to bell shapes, with a smooth surface and displayed a typical A-type crystalline structure. Compared with MS and CS, JSS had higher amylose content, higher RS content and more ordered semi-crystalline lamellae. According to the DSC measurement, JSS had the highest $T_o$. This might be because of the reduced swelling of the granule, probably due to more amylose-lipid complexes with higher amylose content and to its smaller granules which were more resistance to heat. JSS and CS had similar $\Delta H$, due to their similar relative crystallinity. From the pasting property study, the BDV of JSS was lower than those of CS and MS while FV and SBV were higher. Lower BDV might indicate longer amylopectin

chains of JSS, which needs further investigation. As seen from SEM, the degree of digestion of starch followed the order: MS > CS > JSS. Digestion of JSS only apparently occurred at the surface, with a less smooth and more rugged granule surface with occasional pitting. In the course of digestion, for JSS, the scattering intensity and the relative crystallinity were decreased slightly, and the birefringence intensity remained almost the same. These observations indicate the more ordered semi-crystalline lamellae and high relative crystallinity were the major factors for the stronger anti-enzymatic capability of JSS than those of CS and MS. In conclusion, the results presented the detailed related supramolecular structure changes (especially granular, crystalline, and lamellae structure) of JSS granules that control the susceptibility of starch to enzymatic hydrolysis and the physicochemical properties. The knowledge obtained from this work is expected to facilitate further research on the nutritional and other properties of JSS for widening its industrial application.

## 5. Acknowledgments

This research has been financially supported under various projects by the Key Project of the National Natural Science Foundation of China (NSFC) (No.31130042), NSFC-Guangdong Joint Foundation Key Project (No. U1501214), NSFC (No.31271824), YangFan Innovative and Entepreneurial Research Team Project (No. 2014YT02S029), the Ministry of Education Special R&D Funds for the Doctoral Discipline Stations in Universities (20120172110014), the Ministry of Education Program for Supporting New Century Excellent Talents (NCET-12-0193), the Key R&D Projects of Zhongshan (2014A2FC217), the R&D Projects of Guangdong Province (2014B090904047), and the Fundamental Research Funds for the Central Universities (2015ZZ106).

452

453 **References**

454 Asp, N.-G., & Björck, I. (1992). Resistant starch. *Trends in Food Science & Technology, 3*,
455 111-114.

456

457 Blazek, J., & Gilbert, E.P. (2010). Effect of enzymatic hydrolysis on native starch granule
458 structure. *Biomacromolecules, 11*(12), 3275-3289.

459

460 Bobbio, F., EI-Dash, A., Bobbio, P., & Rodrigues, L. (1978). Isolation and characterization of
461 the physicochemical properties of the starch of jackfruit seeds (Artocarpus heterophyllus). *Cereal*
462 *Chemistry*.

463

464 Cameron, R.E., & Donald, A.M. (1992). A small-angle X-ray scattering study of the annealing
465 and gelatinization of starch*.

466

467 Cameron, R.E., & Donald, A.M. (1993a). A small-angle X-ray scattering study of the
468 absorption of water into the starch granule. *Carbohydrate Research, 244*(2), 225-236.

469

470 Cameron, R.E., & Donald, A.M. (1993b). A small‐angle x‐ray scattering study of starch
471 gelatinization in excess and limiting water. *Journal of Polymer Science Part B: Polymer Physics,*
472 *31*(9), 1197-1203.

473

474 Charles, A.L., Chang, Y.H., Ko, W.C., Sriroth, K., & Huang, T.C. (2004). Some physical and
475 chemical properties of starch isolates of cassava genotypes. *Starch - Stärke, 56*(9), 413-418.
476
477 Chiotelli, E., & Le Meste, M. (2002). Effect of small and large wheat starch granules on
478 thermomechanical behavior of starch. *Cereal chemistry, 79*(2), 286-293.
479
480 Chrastil, J. (1987). Improved colorimetric determination of amylose in starches or flours.
481 *Carbohydrate Research, 159*(1), 154-158.
482
483 Colonna, P., Leloup, V., & Buleon, A. (1992). Limiting factors of starch hydrolysis. *European*
484 *journal of clinical nutrition, 46*, S17-32.
485
486 Cooke, D., & Gidley, M.J. (1992). Loss of crystalline and molecular order during starch
487 gelatinisation: origin of the enthalpic transition. *Carbohydrate Research, 227*, 103-112.
488
489 Copeland, L., Blazek, J., Salman, H., & Tang, M.C. (2009). Form and functionality of starch.
490 *Food Hydrocolloids, 23*(6), 1527-1534.
491
492 Crowe, T.C., Seligman, S.A., & Copeland, L. (2000). Inhibition of enzymic digestion of
493 amylose by free fatty acids in vitro contributes to resistant starch formation. *The Journal of*
494 *nutrition, 130*(8), 2006-2008.
495

496 Cui, R., & Oates, C. (1999). + The effect of amylose–lipid complex formation on enzyme
497 susceptibility of sago starch. *Food Chemistry, 65*(4), 417-425.
498
499 Dona, A.C., Pages, G., Gilbert, R.G., & Kuchel, P.W. (2010). Digestion of starch: In vivo and in
500 vitro kinetic models used to characterise oligosaccharide or glucose release. *Carbohydrate*
501 *Polymers, 80*(3), 599-617.
502
503 Englyst, H.N., & Hudson, G.J. (1996). The classification and measurement of dietary
504 carbohydrates. *Food Chemistry, 57*(1), 15-21.
505
506 Englyst, H.N., Kingman, S., & Cummings, J. (1992). Classification and measurement of
507 nutritionally important starch fractions. *European journal of clinical nutrition, 46*, S33-50.
508
509 Fuwa, H., Takaya, T., Sugimoto, Y., & Marshall, J. (1980). Mechanisms of Saccharide
510 Polymerisation and Depolymerisation'. Academic Press, New York.
511
512 Han, X.-Z., & Hamaker, B.R. (2001). Amylopectin fine structure and rice starch paste
513 breakdown. *Journal of Cereal Science, 34*(3), 279-284.
514
515 Hermans, P., & Weidinger, A. (1948). Quantitative X ‐ Ray Investigations on the Crystallinity
516 of Cellulose Fibers. A Background Analysis. *Journal of Applied Physics, 19*(5), 491-506.
517

518 Hizukuri, S. (1985). Relationship between the distribution of the chain length of amylopectin
519 and the crystalline structure of starch granules. *Carbohydrate Research, 141*(2), 295-306.
520
521 ISO. (2007). 6647-2:Rice—Determination of amylose content—Part 2.
522
523 Jane, J., Chen, Y., Lee, L., McPherson, A., Wong, K., Radosavljevic, M., & Kasemsuwan, T.
524 (1999). Effects of amylopectin branch chain length and amylose content on the gelatinization and
525 pasting properties of starch 1. *Cereal chemistry, 76*(5), 629-637.
526
527 Jenkins, D.J., Vuksan, V., Kendall, C.W., Wu¨ rsch, P., Jeffcoat, R., Waring, S., Mehling, C.C.,
528 Vidgen, E., Augustin, L.S., & Wong, E. (1998). Physiological effects of resistant starches on fecal
529 bulk, short chain fatty acids, blood lipids and glycemic index. *Journal of the American College of*
530 *Nutrition, 17*(6), 609-616.
531
532 Karkalas, J., & Raphaelides, S. (1986). Quantitative aspects of amylose-lipid interactions.
533 *Carbohydrate Research, 157*, 215-234.
534
535 Kaur, L., Singh, N., & Sodhi, N.S. (2002). Some properties of potatoes and their starches II.
536 Morphological, thermal and rheological properties of starches. *Food Chemistry, 79*(2), 183-192.
537
538 Kittipongpatana, O.S., & Kittipongpatana, N. (2011). Preparation and physicochemical
539 properties of modified jackfruit starches. *LWT-Food Science and Technology, 44*(8), 1766-1773.

Larson, S.B., Day, J.S., & McPherson, A. (2010). X-ray crystallographic analyses of pig pancreatic α-amylase with limit dextrin, oligosaccharide, and α-cyclodextrin. *Biochemistry, 49*(14), 3101-3115.

Li, X.-j., & Zhong, M. (2004). Study on Granular Morphology of Starch Isolated from Jack-fruit Seeds. *Food Science, 6*, 012.

Madruga, M.S., de Albuquerque, F.S. M., Silva, I.R. A., do Amaral, D.S., Magnani, M., & Neto, V.Q. (2014). Chemical, morphological and functional properties of Brazilian jackfruit (Artocarpus heterophyllus L.) seeds starch. *Food chemistry, 143*, 440-445.

Noda, T., Takahata, Y., Sato, T., Suda, I., Morishita, T., Ishiguro, K., & Yamakawa, O. (1998). Relationships between chain length distribution of amylopectin and gelatinization properties within the same botanical origin for sweet potato and buckwheat. *Carbohydrate Polymers, 37*(2), 153-158.

Oates, C.G. (1997). Towards an understanding of starch granule structure and hydrolysis. *Trends in Food Science & Technology, 8*(11), 375-382.

Planchot, V., Colonna, P., Gallant, D., & Bouchet, B. (1995). Extensive degradation of native starch granules by alpha-amylase from Aspergillus fumigatus. *Journal of Cereal Science, 21*(2), 163-171.

562

563 Pycia, K., Juszczak, L., Gałkowska, D., & Witczak, M. (2012). Physicochemical properties of
564 starches obtained from Polish potato cultivars. *Starch - Stärke, 64*(2), 105-114.

565

566 Rengsutthi, K., & Charoenrein, S. (2011). Physico-chemical properties of jackfruit seed starch
567 (Artocarpus heterophyllus) and its application as a thickener and stabilizer in chilli sauce.
568 *LWT-Food Science and Technology, 44*(5), 1309-1313.

569

570 Robertson, G.H., Wong, D.W., Lee, C.C., Wagschal, K., Smith, M.R., & Orts, W.J. (2006).
571 Native or raw starch digestion: a key step in energy efficient biorefining of grain. *Journal of*
572 *agricultural and food chemistry, 54*(2), 353-365.

573

574 Sarikaya, E., Higasa, T., Adachi, M., & Mikami, B. (2000). Comparison of degradation abilities
575 of α-and β-amylases on raw starch granules. *Process Biochemistry, 35*(7), 711-715.

576

577 Sasaki, T., Yasui, T., & Matsuki, J. (2000). Effect of amylose content on gelatinization,
578 retrogradation, and pasting properties of starches from waxy and nonwaxy wheat and their F1 seeds.
579 *Cereal chemistry, 77*(1), 58-63.

580

581 Shi, Y.-C., & Seib, P.A. (1995). Fine structure of maize starches from four wx-containing
582 genotypes of the W64A inbred line in relation to gelatinization and retrogradation. *Carbohydrate*
583 *Polymers, 26*(2), 141-147.

584

585 Srichuwong, S., Sunarti, T.C., Mishima, T., Isono, N., & Hisamatsu, M. (2005a). Starches from
586 different botanical sources I: Contribution of amylopectin fine structure to thermal properties and
587 enzyme digestibility. *Carbohydrate Polymers, 60*(4), 529-538.

588

589 Srichuwong, S., Sunarti, T.C., Mishima, T., Isono, N., & Hisamatsu, M. (2005b). Starches from
590 different botanical sources II: Contribution of starch structure to swelling and pasting properties.
591 *Carbohydrate Polymers, 62*(1), 25-34.

592

593 Svihus, B., Uhlen, A.K., & Harstad, O.M. (2005). Effect of starch granule structure, associated
594 components and processing on nutritive value of cereal starch: A review. *Animal Feed Science and*
595 *Technology, 122*(3-4), 303-320.

596

597 Tester, R., Qi, X., & Karkalas, J. (2006). Hydrolysis of native starches with amylases. *Animal*
598 *Feed Science and Technology, 130*(1), 39-54.

599

600 Tester, R.F., & Morrison, W.R. (1990). Swelling and gelatinization of cereal starches. I. Effects
601 of amylopectin, amylose, and lipids. *Cereal Chem, 67*(6), 551-557.

602

603 Theivasanthi, T., & Alagar, M. (2011). An insight analysis of nano sized powder of jackfruit
604 seed. *arXiv preprint arXiv:1110.0346*.

605

606 Tufvesson, F., Skrabanja, V., Björck, I., Elmståhl, H.L., & Eliasson, A.-C. (2001). Digestibility
607 of starch systems containing amylose–glycerol monopalmitin complexes. *LWT-Food Science and*
608 *Technology, 34*(3), 131-139.
609
610 Tulyathan, V., Tananuwong, K., Songjinda, P., & Jaiboon, N. (2002). Some physicochemical
611 properties of jackfruit (Artocarpus heterophyllus Lam) seed flour and starch. *Science Asia, 28*,
612 37-41.
613
614 Valetudie, J.C., Colonna, P., Bouchet, B., & Gallant, D.J. (1993). Hydrolysis of Tropical Tuber
615 Starches by Bacterial and Pancreatic α - Amylases. *Starch - Stärke, 45*(8), 270-276.
616
617 Vandeputte, G., Derycke, V., Geeroms, J., & Delcour, J. (2003). Rice starches. II. Structural
618 aspects provide insight into swelling and pasting properties. *Journal of Cereal Science, 38*(1),
619 53-59.
620
621 Vasanthan, T., & Bhatty, R. (1996). Physicochemical properties of small-and large-granule
622 starches of waxy, regular, and high-amylose barleys. *Cereal chemistry, 73*(2), 199-207.
623
624 Vermeylen, R., Goderis, B., & Delcour, J.A. (2006). An X-ray study of hydrothermally treated
625 potato starch. *Carbohydrate Polymers, 64*(2), 364-375.
626
627 Yi, L.X. H. C. H., & Shenghong, C.H. X. (2006). Starch Extraction and Its Characteristics of

628 Jack-fruit Seeds [J]. *Food and Fermentation Industries, 10*, 032.

629

630 Zhang, G., Ao, Z., & Hamaker, B.R. (2006). Slow Digestion Property of Native Cereal Starches.
631 *Biomacromolecules, 7*(11), 3252-3258.

632

633 Zhou, Y., Hoover, R., & Liu, Q. (2004). Relationship between α-amylase degradation and the
634 structure and physicochemical properties of legume starches. *Carbohydrate Polymers, 57*(3),
635 299-317.

636

637 Zhu, J., Li, L., Chen, L., & Li, X. (2012). Study on supramolecular structural changes of
638 ultrasonic treated potato starch granules. *Food Hydrocolloids, 29*(1), 116-122.

639

640 Zobel, H. (1964). X-ray analysis of starch granules. *Methods in carbohydrate chemistry, 4*,
641 109-113.

642

643

644

645

646 Figure Captions

647 Fig.1. SEM images of native and hydrolyzed starch residues at 1000× and 3000×magnification

648 Fig.2. Double-logarithmic SAXS patterns of native and hydrolyzed starch residues. (a) jackfruit
649 seed starch (JSS, JSS-20, and JSS-120); (b) cassava starch (CS, CS-20, and CS-120); (c) maize

starch (MS, MS-20, and MS-120).

Fig.3. Polarized light microscopic images of native and hydrolyzed starch residues

Fig.4. XRD patterns of native and hydrolyzed starch residues, (a) jackfruit seed starch (JSS, JSS-20, and JSS-120); (b) cassava starch (CS, CS-20, and CS-120); (c) maize starch (MS, MS-20, and MS-120).

Fig.5. Differential scanning calorimetry (DSC) thermograhs (a), and viscosity curves (b) of jackfruit seed starch, cassava starch and maize starch

Tables

Table 1 Amylose contents and *in vitro* enzyme digestion analysis of jackfruit seed starch (JSS), cassava starch (CS) and maize starch (MS).

| Raw starches | RDS (%) | SDS (%) | RS (%) | Amylose (%) |
|---|---|---|---|---|
| Jackfruit seed starch (JSS) | 5.92±0.49$^{c}$ | 19.82±1.01$^{c}$ | 74.26±1.28$^{a}$ | 24.90±0.10$^{a}$ |
| Cassava starch (CS) | 10.50±0.04$^{b}$ | 38.43±0.03$^{b}$ | 51.07±0.08$^{b}$ | 16.68±0.54$^{c}$ |
| Maize starch (MS) | 12.04±0.04$^{a}$ | 69.73±1.14$^{a}$ | 18.23±1.18$^{c}$ | 22.42±0.19$^{b}$ |

Values are means of three determinations (±standard deviation); values followed by the different letters within a column differ significantly ($p < 0.05$).

665 Table 2. SAXS parameters and relative crystallinity of native and hydrolyzed starches.

| Sample | $q_{peak}$ ($nm^{-1}$) | $d$ (nm) | Peak Area | RC (%) |
|---|---|---|---|---|
| JSS | $0.6934^{abc}$ | $9.06^{de}$ | $0.1288^{a}$ | $30.6^{ab}$ |
| JSS-20 | $0.6868^{bcd}$ | $9.15^{cd}$ | $0.1240^{a}$ | $28.5^{abcd}$ |
| JSS-120 | $0.7001^{ab}$ | $8.98^{de}$ | $0.0653^{c}$ | $27.6^{bcd}$ |
| CS | $0.6868^{bcd}$ | $9.14^{de}$ | $0.1248^{a}$ | $30.3^{ab}$ |
| CS-20 | $0.6802^{cd}$ | $9.24^{c}$ | $0.0639^{c}$ | $25.4^{def}$ |
| CS-120 | $0.6934^{abc}$ | $9.01^{de}$ | $0.0318^{d}$ | $23.6^{efg}$ |
| MS | $0.6670^{e}$ | $9.42^{b}$ | $0.0800^{b}$ | $27.4^{cde}$ |
| MS-20 | $0.6604^{e}$ | $9.51^{b}$ | $0.0572^{c}$ | $21.5^{g}$ |
| MS-120 | $0.6208^{f}$ | $10.12^{a}$ | $0.0213^{d}$ | $19.4^{g}$ |

666 Values are means of three determinations; values followed by the different letters within a column differ significantly ($p$

667 $< 0.05$).

668

669 Table 3 Gelatinization parameters and pasting properties of jackfruit seed starch (JSS), cassava starch (CS) and maize

670 starch (MS)

| Sample | JSS | CS | MS |
|---|---|---|---|
| $T_o$ (°C) | 81.11±0.53[a] | 60.47±1.00[c] | 65.58±0.45[b] |
| $T_p$ (°C) | 85.39±0.64[a] | 65.88±0.78[c] | 69.43±0.15[b] |
| $T_c$ (°C) | 91.70±1.12[a] | 79.32±0.84[b] | 75.48±0.38[c] |
| $\Delta T$ ($T_c$−$T_o$) | 10.59±0.65[b] | 18.85±1.85[a] | 9.90±0.09[b] |
| $\Delta H$ (J/g) | 19.61±0.76[a] | 19.67±0.41[a] | 15.86±0.32[b] |
| PT (°C) | 82.0±0.2[a] | 66.9±0.3[c] | 71.5±0.2[b] |
| PV (mPa·s) | 844.0±5.1[b] | 963.2±4.3[a] | 743.9±3.3[c] |
| BDV (mPa·s) | 109.5±2.4[c] | 473.2±1.5[a] | 288.4±1.8[b] |
| FV (mPa·s) | 1354.0±7.4[a] | 1044.0±6.3[b] | 827.9±5.2[c] |
| SBV (mPa·s) | 548.9±3.5[a] | 514.4±4.1[b] | 349.1±3.8[c] |

671 $T_o$, $T_p$ and $T_c$ correspond to onset, peak and conclusion gelatinization temperature (°C); whereas $\Delta H$ and $\Delta T$ represent

672 melting enthalpy (J/g of starch) and gelatinization temperature range (°C) respectively. PT represents peak temperature

673 (°C), whereas PV, BDV, FV, SBV correspond to peak viscosity, breakdown viscosity, final viscosity and setback

674 viscosity (mPa·s) respectively.

675 Values in the table are means of three determinations (± standard deviation); values followed by the different letters

676 within a column differ significantly ($p < 0.05$).

677

678

679 Figures

680

681

682 Fig 1

683

684

685 Fig 2

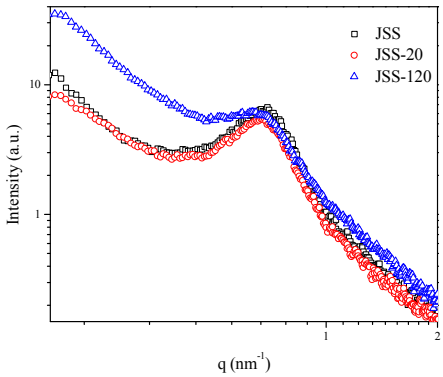


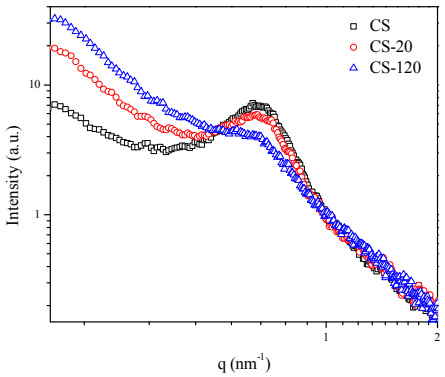


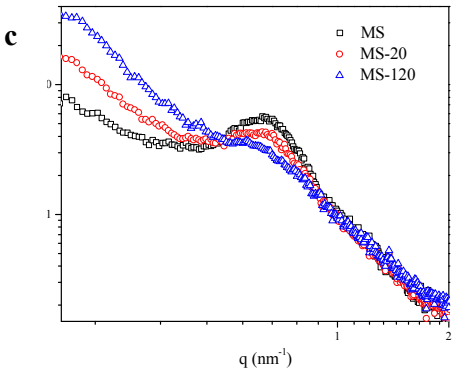


fig 3

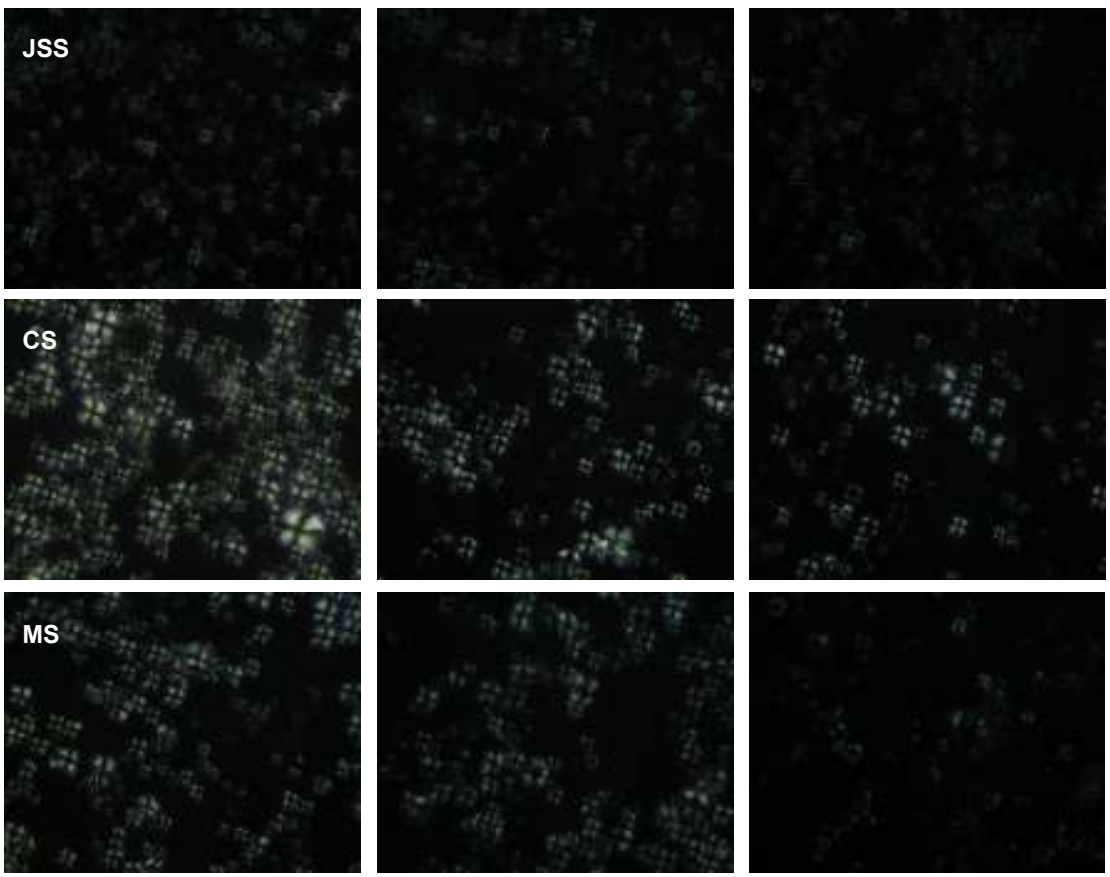

698

699

700 Fig 4

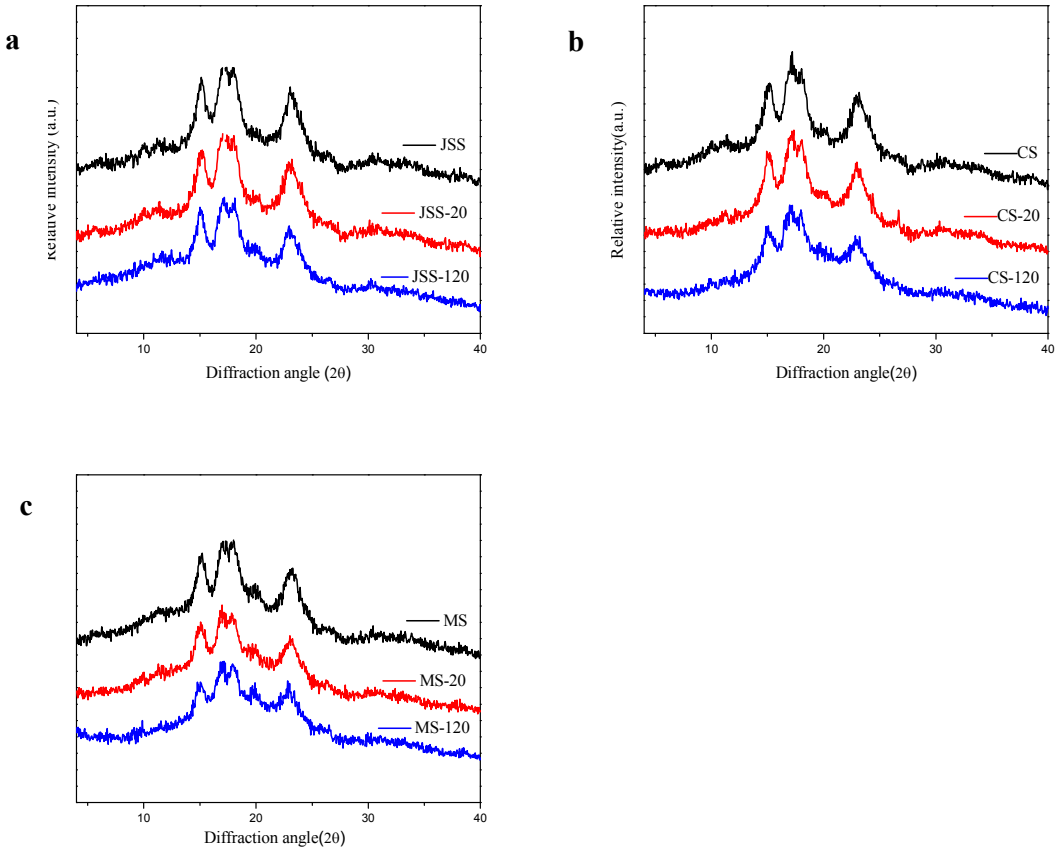


701

702

703

704

705

706

707

708

709

710

711 Fig 5

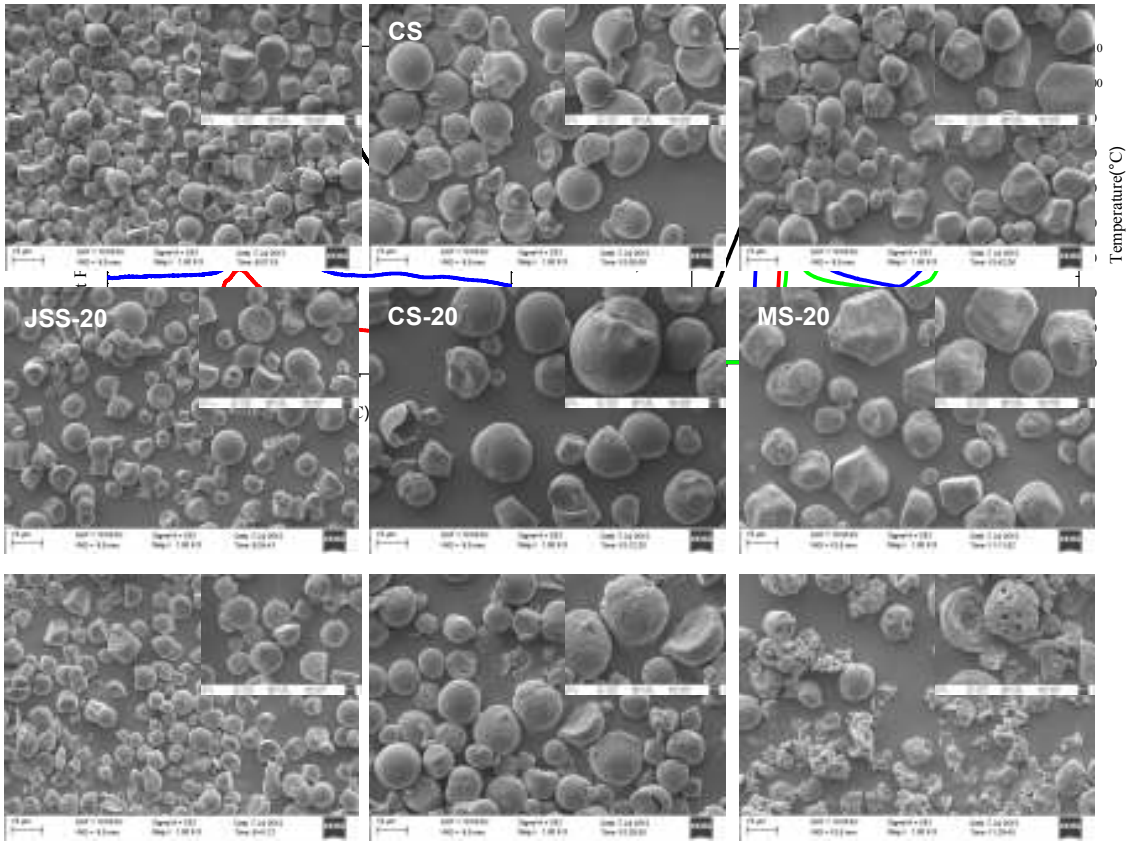


712

713

714

715

716

717

718

719

720